

## Electron-Hole Liquids in Semiconductors

W. F. Brinkman and T. M. Rice

*Bell Telephone Laboratories, Holmdel and Murray Hill, New Jersey*

(Received 1 August 1972)

In this paper the energetics of the formation of electron-hole metallic liquids in semiconductors is examined. The ground-state energies of electron-hole metals are calculated using Hubbard's approximate treatment of the electron gas for the following cases: (a) germanium, (b) germanium with a large (111) strain, (c) silicon, and (d) GaAs. The simple case of a single isotropic maximum for the valence band and a single minimum for the conduction band is also treated. It is shown that for both Si and Ge, the binding energy of the metallic state relative to free excitons is 5.7 and 1.7 meV, respectively. These values and the values of the equilibrium density are in good agreement with experiment. In the isotropic model the metallic state is not bound while for GaAs and strained Ge the metallic-state energy per electron is essentially equal to that for a gas of free excitons. The low-density limit of the isotropic band model is examined and the ground state for this system is predicted to be a dilute gas of molecules. It is argued that the forces between molecules are repulsive and will cause this state to break up at relatively low densities. If the density is increased, the system will undergo a first-order transition to the metallic state. The relevance of these calculations to the metal-insulator transition problem is discussed. It is pointed out that the fact that anisotropic and many-valleyed bands favor the metallic state means that the metal-insulator transition must ultimately be first order.

### I. INTRODUCTION

In the last four years considerable experimental evidence has been accumulating that electrons and holes in Ge and Si undergo a gas-liquid-type transition at low temperatures as a function of density. Such a transition was first suggested by Keldysh,<sup>1</sup> who said that metallized droplets of electrons and holes could form as the density is increased. The first evidence for the existence of such metallic droplets was given by the photoconductivity experiments of Asnin and Rogachev<sup>2</sup> and the observation of shifted recombination radiation attributed to the droplet state by Pokrovsky and Svistunova.<sup>3-8</sup> More conclusive evidence, however, was obtained in the  $p$ - $n$  junction noise experiments performed by Asnin *et al.*<sup>9</sup> and Benoît à la Guillaume *et al.*<sup>10</sup> and in the light-scattering experiments of Pokrovsky and Svistunova.<sup>11</sup> The reason such a phase transition is observable in Ge, in particular, is that the recombination times are of the order of  $5 \times 10^{-6}$  sec because of the indirect gap, while the thermalization times are  $10^{-9}$  sec. One, therefore, has several microseconds in which to study the system of electrons and holes in thermal equilibrium. Experimentally, the binding energy of the liquid state relative to free excitons and its equilibrium density are reasonably well established for Ge and there is some evidence for their values in the presence of strain. Less complete investigations have been carried out on Si. In this paper we shall examine theoretically the energetics of the electron-hole liquid and gaseous states.<sup>12</sup> We shall assume throughout this paper that the "liquid" state is metallic even though this has not been definitely estab-

lished experimentally.

The simple case of a single isotropic band for both the electrons and holes is considered in Sec. II. The interaction between the electrons and holes is assumed to be the Coulomb interaction reduced by the static dielectric constant. This form of the interaction can be justified provided the effective Bohr radius  $a_x$  is large compared to the lattice constant and the fraction of electrons excited into the valence band is small.<sup>13</sup> The ground-state energy has been calculated by using a procedure due to Hubbard<sup>14</sup> based on the random-phase approximation. It is found that for mass ratios not very different from unity the metallic state is not stable relative to the decay into a dilute gas of free excitons. It is difficult to assess the accuracy of the Hubbard approximation but, as discussed in Sec. II, it is thought to be reasonable.

The complications due to the actual band structure of Ge and Si are added to the calculation of the metallic energy in Sec. III. As previously pointed out by Pokrovsky *et al.*,<sup>5</sup> the nature of the band structure considerably reduces the kinetic energy in the metallic state. In calculating the correlation energy we include the degeneracy of bands but not their anisotropy. We find that the metallic state is bound in Ge by 1.7 meV. Experimentally, the binding energy is estimated to be 2.4–2.7 meV. The theoretical equilibrium density in Ge is very close to the experimental value of  $2 \times 10^{17}$  cm<sup>-3</sup>. Calculations for strained Ge and Si are also discussed. Independently, Combescot and Nozières (CN)<sup>15</sup> have performed similar calculations but used the Nozières-Pines<sup>16</sup> treatment of the correlation

energy including the anisotropic masses. Their result for the binding energy is 2.5 meV, in better agreement with experiment. {*Note added in proof.* Recent studies of the temperature dependence of the droplet state in Ge lead to values of binding energy  $\approx 1.4$  meV. Y. E. Pokrovsky [Phys. Status Solidi (a) 11, 385 (1972)] studied the temperature dependence of the luminescence under continuous pumping conditions while J. C. Hensel, T. G. Phillips, and T. M. Rice (unpublished) studied the temperature dependence of the time decay of the cyclotron resonance. The value obtained in these experiments is appreciably lower than the values obtained previously and discussed in the text. The reason for this discrepancy is presently not clear.}

In Sec. III we also calculate the ground-state energy of an electron-hole plasma in GaAs. Even though this is a direct-gap material there is some evidence<sup>17</sup> for metalization of electrons and holes at high pumping powers.

In Sec. IV we discuss the low-density electron-hole gas in the isotropic band model. It is known that two excitons bind to form molecules.<sup>18</sup> The intermolecular potential is estimated assuming the excitons interact in pairs. The scattering length is found to be large and repulsive and, therefore, no gas-liquid transition is predicted for the molecules. As the density is increased the repulsive interaction causes an increase in the ground-state energy and it is possible that a first-order transition to the metallic state could occur.

The relation of the present work to the metal-semiconductor transition<sup>19-21</sup> is discussed in Sec. V. In the presence of anisotropic and degenerate band structures the metallic liquid is lower in energy than free excitons. Therefore as the energy gap in a semiconductor is reduced the system will undergo a first-order phase transition to a semimetallic state when the gap equals the binding energy of the electron-hole metallic liquid. This occurs at a value of the gap larger than the excitonic instability. Thus we find that excitonic phases can occur only for simple band structures.

## II. ISOTROPIC BANDS

We begin our discussion of the electron-hole liquid by considering the simplest case of isotropic-nondegenerate energy bands for the electrons and holes. In the limit that the hole mass  $m_h$  equals the electron mass  $m_e$  the problem is that of a hypothetical gas of electrons and positrons in which the radiative recombination of electrons and positrons is ignored. In the limit  $m_h \gg m_e$ , the problem is equivalent to the metallic phase of hydrogen examined by Wigner and Huntington<sup>22</sup> and others.<sup>23</sup>

The Hamiltonian  $H$  is given by

$$H = \frac{-1}{2m_e} \sum_{i=1}^N \nabla_i^2 - \frac{1}{2m_h} \sum_{j=1}^N \nabla_j^2 + \frac{1}{2} \sum_{i \neq j} \frac{e^2}{\kappa |\vec{r}_i^e - \vec{r}_j^e|} + \frac{1}{2} \sum_{i \neq j} \frac{e^2}{\kappa |\vec{r}_i^h - \vec{r}_j^h|} - \sum_{i,j} \frac{e^2}{\kappa |\vec{r}_i^e - \vec{r}_j^h|}, \quad (2.1)$$

where the first two terms represent the kinetic energies of the electrons and holes and the other terms represent the repulsive Coulomb interactions between like particles and the attractive Coulomb interactions between unlike particles. All of the Coulomb forces are reduced by the static dielectric constant  $\kappa$ . It is convenient to measure energy in units of the binding energy  $E_x$  of an exciton, or single bound electron-hole pair, which is given by the standard hydrogenic formula  $E_x = \mu/m\kappa^2$  Ry where  $\mu$  is the reduced mass,  $\mu^{-1} = m_e^{-1} + m_h^{-1}$ . The corresponding unit of length is the Bohr radius of an exciton which is  $a_x = (m\kappa/\mu)a_0$ . The density of electrons  $n$  can be characterized by the dimensionless parameter  $r_s$ , the radius of a sphere whose volume is equal to  $n^{-1}$  measured in units of  $a_x^3$ .

At high densities, or small values of  $r_s$ , the electron-hole liquid will be metallic. The dominant term in the high-density limit is the kinetic energy of the degenerate electrons and holes which gives a contribution to the ground-state energy per electron,

$$E_k = \frac{3}{5} \left( \frac{k_F^2}{2m_e} + \frac{k_F^2}{2m_h} \right) = \frac{3}{5} \left( \frac{9\pi}{4} \right)^{2/3} \frac{1}{r_s^2} = \frac{2.21}{r_s^2}, \quad (2.2)$$

where  $k_F$  is the Fermi momentum of the electrons. The first correction is the exchange energy which is the expectation value of the potential energy in the ground state of noninteracting electrons and holes:

$$E_{ex} = - \frac{3e^2}{2\pi\kappa} k_F = - \frac{3}{\pi} \left( \frac{9\pi}{4} \right)^{1/3} \frac{1}{r_s} = - \frac{1.832}{r_s}. \quad (2.3)$$

Note that the electrons and holes make equal contributions to the exchange energy irrespective of the mass ratio  $m_h/m_e$ . The remaining contribution is called the correlation energy. Hanamura<sup>24</sup> has used the high-density expansion, which is valid for  $r_s \ll 1$ , to estimate this term. However, it is known from the study of the single-component electron gas that such expansions are limited to values of  $r_s < 1$  and, as we shall see, the relevant values of  $r_s$  here are  $r_s > 1$ . Several schemes<sup>14,16</sup> based on the random-phase approximation (RPA) have been developed to estimate the correlation energy of the single-component electron gas in the intermediate density regime  $1 \lesssim r_s \lesssim 5$ . These procedures, although lacking a rigorous justification, give good agreement when compared with the experiment on nearly-free-electron metals.<sup>25</sup> Since the various estimates of the correlation energy of the electron gas do not differ appreciably,

we shall use the approximation scheme put forward by Hubbard for the single-component electron gas. The exact expression for the correlation energy is

$$E_c = -\frac{1}{2\pi n} \int_0^1 \frac{d\lambda}{\lambda} \int \frac{d^3k}{(2\pi)^3} \int_0^\infty d\omega \operatorname{Im}[\epsilon_\lambda^{-1}(k, \omega)] - E_{\text{ex}} - 2 \int \frac{d^3k}{(2\pi)^3} \frac{2\pi e^2}{k^2}. \quad (2.4)$$

The dielectric constant  $\epsilon_\lambda(k, \omega)$  can be expressed in terms of the total polarizability. The  $\lambda$  integral is over the coupling constant  $\lambda e^2$ . In the RPA the total polarizability is given by the sum of the polarizabilities of the electrons  $\pi^e$  and the holes  $\pi^h$ , so that

$$\epsilon_\lambda(\vec{k}, \omega) = 1 - [\pi^e(\vec{k}, \omega) + \pi^h(\vec{k}, \omega)]. \quad (2.5)$$

The RPA polarizability  $\pi_{\text{RPA}}$  is given by the Lindhard function

$$\pi_{\text{RPA}}^e(\vec{k}, \omega) = -\frac{4\pi e^2 \lambda}{\kappa k^2} \sum_{p, \sigma} \frac{n_{\vec{p}+\vec{k}, \sigma} - n_{\vec{p}, \sigma}}{\omega + [p^2 - (\vec{p} + \vec{k})^2]/2m^e + i\delta}, \quad (2.6)$$

where  $n_{\vec{p}\sigma} = 1$ ,  $p < p_F$ , and  $n_p = 0$  otherwise. At short wavelengths, or  $k \gg k_F$  in Eq. (2.4), the RPA result for the correlation energy is seriously in error, since it treats the correlations between particles on an equal footing irrespective of their spin states. However, electrons or holes with parallel spins are kept apart by the Pauli exclusion principle and thus do not contribute to the correlation energy at large  $k$ . Hubbard<sup>14</sup> and Nozières and Pines<sup>16</sup> have proposed modifications of the RPA to take account of this fact. We shall follow the scheme proposed by Hubbard. He showed that one could approximately include the diagrams that are the exchange conjugates of the RPA bubble diagrams by replacing  $\pi_{\text{RPA}}$  by  $\pi_H$ , where

$$\pi_H(k, \omega) = \frac{\pi_{\text{RPA}}(k, \omega)}{1 + f(k)\pi_{\text{RPA}}(k, \omega)}, \quad (2.7)$$

where  $f(k) = 0.5k^2/(k^2 + k_F^2)$ . We can generalize his arguments straightforwardly to the multicomponent system by making the replacement (2.7) separately for each component. This complicates the integration over the coupling constant in (2.4).

In the equal-mass limit,  $\pi^e \equiv \pi^h$  and the correlation energy can be expressed after a little algebra as

$$E_c = -\frac{1}{4\pi n} \int \frac{d^3k}{(2\pi)^3} \int_0^\infty d\omega \left( \frac{2\Sigma(k, \omega)}{\Sigma'(k, \omega)} \tan^{-1} \frac{\Sigma'(k, \omega)}{1 - A'(k, \omega)} - 2\Sigma(k, \omega) \right), \quad (2.8)$$

where  $\pi = A + i\Sigma$  and  $\Sigma' = [2 - k^2/2(k^2 + k_F^2)]\Sigma$  and  $A'/A = \Sigma'/\Sigma$ . Note that the exchange contributions

play a less important role than in the single-component electron gas and cancel only one-fourth of the RPA correlation energy at large  $k$ . The results for the correlation energy are tabulated in Table I and, in Fig. 1, the total ground-state energy  $E_G$  is plotted vs  $r_s$ . The results show a minimum in  $E_G(r_s)$  at a value of  $r_s = 1.95$  with a minimum value of  $E_G^0 = -0.86$ . This value is considerably lower than the minimum value of  $E_G^0 = -0.35$  at  $r_s = 1.7$  found by Hanamura.<sup>24</sup> However, the minimum value lies substantially above the energy of free excitons so that within our approximation scheme we do not find the metallic state bound relative to free excitons for equal masses.

When the electron and hole masses are unequal, the substitution (2.7) leads to a complicated expression for the integrand in Eq. (2.4). Since the exchange correction is small in this problem, we approximate it by making the substitution in Eq. (2.8) of

$$\Sigma' = \left( 1 - \frac{k^2}{4(k^2 + k_F^2)} \right) (\Sigma^e + \Sigma^h), \quad 2\Sigma = \Sigma^e + \Sigma^h, \quad (2.9)$$

and again set  $A'/A = \Sigma'/\Sigma$ . We have evaluated the correlation energy for a range of values of  $m_e/m_h$ . In Fig. 2 we plot the results obtained in this way for the minimum ground-state energy in units of the exciton rydberg. We see that it decreases slowly as the ratio  $m_e/m_h$  decreases. The equilibrium value of  $r_s$  stays almost constant and varies only from  $r_s = 1.95$  at  $m_e/m_h = 1$  to a value  $r_s = 1.7$  at  $m_e/m_h = 0.1$ . Note that the absolute units of energy and length change by a factor of 2 in going from  $m_e/m_h = 1$  to  $m_e/m_h = 0$ .

It is interesting to compare our results with the calculated values of the ground-state energy of metallic hydrogen. The Wigner-Seitz method has been applied by Wigner and Huntington<sup>22</sup> and by Kronig, de Boer, and Korringa<sup>26</sup> to the hypothetical metallic state of  $H$ . Wigner and Huntington find the energy can be written as

$$E_G^0 = -1.05 + 0.8(m_e/m_h)^{1/2}, \quad (2.10)$$

with an equilibrium value of  $r_s = 1.63$ . Their results are shown in Fig. 2. The square-root de-

TABLE I. Correlation energy at different values of  $r_s$ .

	$r_s = 0.5$	1.0	1.5	2.0	2.5
$m_e/m_h = 1$	-0.67	-0.56	-0.49	-0.44	-0.44
1.5	-0.68	-0.57	-0.50	-0.45	-0.45
2	-0.70	-0.58	-0.51	-0.45	-0.45
4	-0.76	-0.63	-0.55	-0.49	-0.49
10	-0.92	-0.75	-0.65	-0.57	-0.57
Ge	-1.52	-1.07	-0.86	-0.73	-0.64
Si	-1.64	-1.12	-0.89	-0.76	-0.65
Ge with [111] strain	-0.84	-0.69	-0.59	-0.53	-0.53

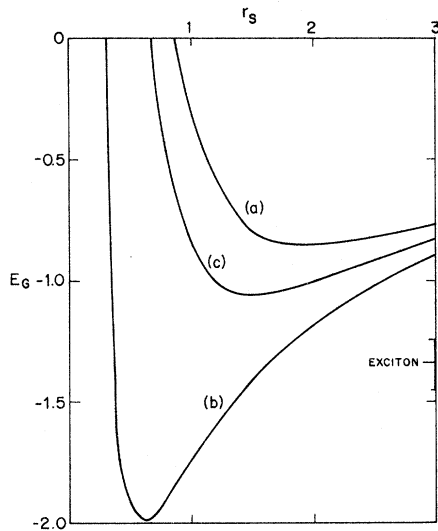


FIG. 1. Ground-state energy plotted against  $r_s$ . (a) Isotropic model with one maximum in the valence band and one minimum in the conduction band; (b) germanium; and (c) germanium under a large (1,1,1) strain. The parameters used are listed in Table II. The bar on the right indicates experimental binding of the lowest exciton in Ge. The width is the experimental error.

pendence on the mass ratio arises from the zero-point motion of the positive charged particles and is sufficiently large to cause the metallic phase to be unbound relative to free excitons for values of  $m_e/m_h > 1/256$ . It is clear from Fig. 2 that our modified RPA calculations account qualitatively for the correct trends as the mass ratio  $m_e/m_h$  decreases. However, it is also clear that they break down as  $m_e/m_h$  becomes very small. It

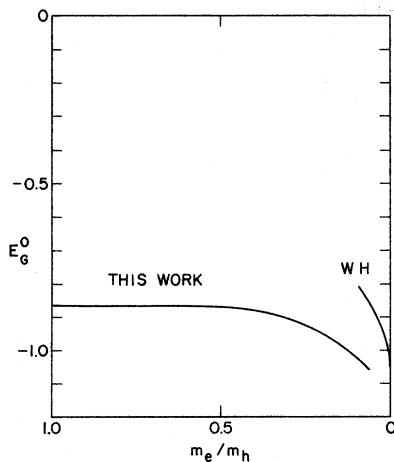


FIG. 2. Minimum energy plotted against the mass ratio  $m_e/m_h$ . The curve labeled WH is obtained from the work of Wigner and Huntington. The other curve is obtained from Eq. (2.8) using (2.9).

should also be pointed out that  $E_G^0(m_e/m_h)$  cannot be an analytic function in the interval  $0 < m_e/m_h < 1$ , since as  $m_e/m_h$  increases from zero the lattice of positively charged particles must melt, which leads to first-order phase transition and a discontinuity in slope of  $E_G^0$  at the critical value of  $m_e/m_h$ .

One major weakness of our calculations is that they do not have the property in the low-density limit,  $\lim_{r_s \rightarrow \infty} E_G(r_s) \rightarrow -1$  as  $r_s \rightarrow \infty$ , the energy of free excitons. This is not surprising since we have omitted the terms corresponding to the multiple scattering of an electron and a hole, which give rise to the exciton bound states. Within our approximation scheme the second-order correlation-energy graphs shown on Figs. 3(a) and 3(b) are included, though the latter are only approximated. However, while the Hubbard correction includes 3(c) and approximates graphs 3(e) and 3(f) in third order, it ignores completely graphs 3(d) and self-energy corrections to one-particle propagators. As the density is lowered, the electron-hole correlations typified by these higher-order graphs become increasingly important. We can make an estimate of their importance in several ways. One is to use the Mott criterion<sup>27</sup> for the metal-nonmetal transition. This criterion is the condition for the occurrence of a bound state of an electron and a hole interacting via the screened Coulomb potential. Such a bound state will not occur for

$$q_{\text{FT}} > 1/a_x, \quad (2.11)$$

where  $q_{\text{FT}}$  is the Fermi-Thomas screening vector.<sup>25</sup> For equal masses  $q_{\text{FT}}^2 = 8me^2n^{1/3}/\kappa$  and when substituted in Eq. (2.11) leads to criterion  $r_s < 9.9$ . This value is a factor of 4 larger in  $r_s$  than in the case of hydrogen (or  $m_e/m_h = 0$ ). The difference arises both from the extra screening in the presence of two types of carriers and from the greater difficulty in localizing an electron and a hole simultaneously. Clearly the equilibrium value  $r_s \approx 2$  is well away from the Mott criterion.

An alternative method of examining the role of

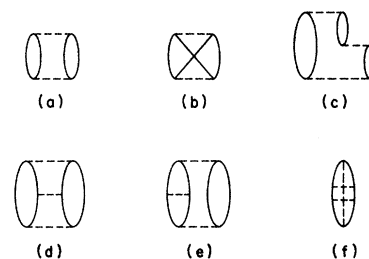


FIG. 3. Various diagrams occurring in second and third order in perturbation theory. Diagrams of the type (d) are not included in the Hubbard approximation.

the ladder graphs is to evaluate the contribution to the ground-state energy from the electron-hole pairing instability at very low temperatures.<sup>28</sup> For isotropic bands the Fermi surfaces of the electrons and the holes are identical and the system is unstable at any density at zero temperature towards the formation of electron-hole pairs. This instability has been discussed by several authors<sup>20,21,28</sup> and arises from a divergence of the repeated electron-hole scattering diagrams in the metallic state. In Appendix A we estimate the contribution to the ground-state energy associated with phase transition to the paired state as a function of density. It is very small for values of  $r_s \sim 2$ . Indeed for  $r_s < 8$  it contributes less than 2% to the ground-state energy.

The small size of this binding energy does not, however, give any direct evidence on the importance of the multiple electron-hole scattering in renormalizing the electron density near a hole. One can see this by noting that, if for a single positron in an electron gas we use the criterion (2.11) for the formation of positronium, the critical value is again  $r_s = 9.9$ , where  $r_s$  is measured in conventional Bohr radii. However, it is known<sup>29</sup> that electron-positron correlations are quite important throughout the range of  $2 < r_s < 5$ . A considerable amount of electron-hole correlation is included already within the RPA. This is illustrated by calculating the electron-hole correlation function  $g_{eh}(r)$ . The details are given in Appendix B. In Fig. 4 we plot  $g_{eh}(r)$  obtained in the RPA for a value of  $r_s = 1$ . We see that there is substantial enhancement of  $g_{eh}(r)$  at small  $r$ . The enhanced density of electrons at the holes is  $3g_{eh}(0)/4\pi r_s^3$  and may be compared to the density in the exciton wave function of  $\pi^{-1}$ . For the equilibrium value of  $r_s \approx 2$  we estimate  $g_{eh}(0) \approx 3$ , so that the ratio is

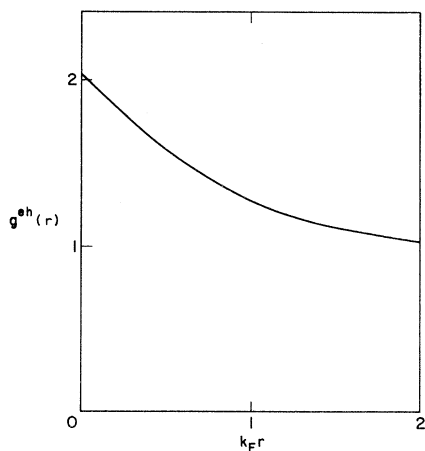


FIG. 4. Electron-hole correlation function plotted vs distance in units of the Fermi wave vector  $r_s = 1$ .

$3g_{eh}(0)/4r_s^3 = 0.28$ . This value is much less than unity. At first sight this result is disturbing. It is known from positron-annihilation studies in the alkali metals that electron density at the positron is larger than in positronium.<sup>29</sup> In Na, where the electronic density is approximately equal to the equilibrium value, we find for the electron-positron liquid, the experiments of Weisberg and Berko<sup>30</sup> show an enhancement of 50% over positronium, which gives an enhancement of a factor of 16 over the uniform electron density. It is clear, however, that on passing from the one-positron to the many-positron problem the kinetic energy of the positrons will reduce the enhancement. A large number of positrons also presents the electron gas with an averaged potential that is lowered. Therefore, the electrons do not gain as much energy by clustering around the positrons as they would for a single positron. A more relevant comparison, perhaps, is to the electronic density at the proton in the metallic state of hydrogen. In a Wigner-Seitz calculation the electron-proton correlation is treated accurately by solving for the wave function  $\psi_0(r)$  of an electron moving in the attractive potential of the proton subject to the boundary condition that  $\partial\psi/\partial r|_{r=r_p} = 0$  on the Wigner-Seitz sphere. Kronig, de Boer, and Korringa<sup>26</sup> found an approximate solution for  $\psi_0(r)$  and we find using their result that the electron density at the proton is a factor of 2.2 larger than the uniform density. This leads to a value of 0.38 for the ratio of charge density at the proton in the metal to that in a hydrogen atom. This value is only slightly larger than the value we found at equilibrium ignoring multiple electron-hole scattering. These calculations indicate that there is much less correlation in the metallic states than in the corresponding atomic or molecular states leading to much reduced values for both kinetic and potential energies. They also pose the difficult question of whether there are much more strongly correlated, and presumably insulating, states that are lower in energy in the range  $r_s \sim 1.5-2$  than the metallic state we have calculated. We defer further consideration of this question to Sec. IV.

### III. EFFECTS OF THE BAND STRUCTURE

Thus far in this paper, we have limited the discussion to an ideal model with isotropic electron and hole bands. However, in the semiconductors of interest the detailed form of the electron and hole bands is known very accurately and is highly anisotropic and far from the ideal behavior. We shall present here detailed calculations in four cases of experimental interest: (a) germanium, (b) silicon, (c) germanium in the presence of a [111] strain that is large enough to completely remove the degeneracies of the electron and the

hole bands, and (d) a direct gap semiconductor, GaAs.

#### A. Germanium

In Ge, the minima in the electron (or conduction) band are ellipsoidal in shape and are located at the  $L$  point of the zone. There are four equivalent electron ellipsoids. From cyclotron-resonance studies, the transverse ( $m_t$ ) and longitudinal ( $m_l$ ) masses are known accurately and their values are  $m_t = 0.082m$  and  $m_l = 1.58m$ .<sup>31</sup> The hole (or valence) band structure consists of two bands which are degenerate  $\Gamma_8$  levels at the center of the zone, but which are split into heavy- and light-hole bands away from  $\Gamma$ . The detailed form of the energy eigenvalues is

$$E^\pm(\vec{k}) = Ak^2 \pm [B^2k^4 + C^2(k_x^2k_y^2 + k_y^2k_z^2 + k_z^2k_x^2)]^{1/2}. \quad (3.1)$$

For the parameters  $A$ ,  $B$ , and  $C$  we use the latest values from the cyclotron-resonance work of Hansel and Suzuki<sup>32</sup> quoted in Table II.

The anisotropies and degeneracies in the band structure both tend to stabilize the metallic phase. This can be seen in the first place by examining the kinetic energy. The kinetic energy per electron is proportional to the Fermi energy  $E_F^e$  [see Eq. (2.2)] and distributing the electrons among four ellipsoids lowers the Fermi energy by a factor  $4^{2/3}$ . Secondly, it is straightforward to show that the mass that enters the Fermi energy is the geometric mean over the three principal directions of the ellipsoids. Denoting this density-of-states mass for the electron as  $m_{de}$ , we find

$$m_{de} = m_t^{2/3} m_l^{1/3} = 0.22 \text{ (Ge)}. \quad (3.2)$$

On the other hand, if we use the usual  $1s$  function as a trial wave function in an exciton, the reciprocally averaged, or optical, mass enters:

$$m_{oe}^{-1} = \frac{1}{3} (2m_t^{-1} + m_l^{-1}), \quad m_{oe} = 0.12 \text{ (Ge)}. \quad (3.3)$$

Thus the kinetic energy has a heavier mass, and therefore a lower value, in the metallic state than in free excitons.

A similar effect is found for the holes. The number of states per unit volume  $n_h(\epsilon)$  below an energy  $\epsilon$  in the hole bands is

$$n_h(\epsilon) = \frac{2}{8\pi^3} \int d^3k [\theta(\epsilon - E^+(\vec{k})) + \theta(\epsilon - E^-(\vec{k}))]. \quad (3.4)$$

Expressing  $\vec{k}$  in polar coordinates  $(k, \theta, \phi)$ , one

sees that in a given direction  $(\theta, \phi)$  the bands (3.1) are parabolic and the effect of the degeneracy is to cause a cubic warping as a function of angle. Thus in a given direction the integral over  $k$  may be done at once and we find

$$n_h(\epsilon) = \frac{1}{12\pi^3} \int_{-1}^{+1} d(\cos\theta) \int_0^{2\pi} d\phi [k_+^3(\theta, \phi) + k_-^3(\theta, \phi)], \quad (3.5)$$

where

$$k_\pm^2(\theta, \phi) = \epsilon \{A \pm [B^2 + C^2\psi(\theta, \phi)]^{1/2}\}^{-1} \quad (3.6)$$

and

$$\psi(\theta, \phi) = \sin^4\theta \cos^2\phi \sin^2\phi + \sin^2\theta \cos^2\theta. \quad (3.7)$$

Defining a light ( $m_{lh}$ ) and heavy ( $m_{hh}$ ) hole mass corresponding to the first and second terms in Eq. (3.5) by

$$n_h(\epsilon) = \frac{(2\epsilon)^{3/2}}{3\pi^2} (m_{lh}^{3/2} + m_{hh}^{3/2}), \quad (3.8)$$

we obtain values of  $m_{lh} = 0.042m$  and  $m_{hh} = 0.347m$  by numerical integration of Eq. (3.5). [Note that our value of  $m_{hh}$  is larger than the value of CN, who used the approximation  $(2m_{hh})^{-1} = A - (B^2 + \frac{1}{6}C^2)^{1/2}$  and obtain a value  $m_{hh} = 0.30m$ .] Again there is a large difference between the reciprocally averaged or optical mass  $m_{oh} (= A^{-1} = 0.07m)$  and the heavy hole mass  $m_{hh}$  which dominates in the kinetic energy of the metallic state. From the optical effective masses we can define a reduced mass  $\mu$  as  $\mu^{-1} = m_{oe}^{-1} + m_{oh}^{-1}$  and in Ge we obtain  $\mu = 0.046m$  which, when combined with the dielectric constant  $\kappa = 15.36$  in Ge, yields an approximate exciton binding energy of  $E_{Ge}^x = 2.65$  meV. This value is smaller than the latest<sup>33</sup> experimental values of  $3.6 \pm 0.3$  and  $2.8 \pm 0.3$  meV for the two excitons in Ge. Accurate theoretical calculations including the anisotropies yield theoretical values in excellent agreement with the experimental numbers.<sup>34</sup> We wish again to point out the difference between average masses entering the kinetic energy in the metal and the exciton. If we use  $m_{de}$  and  $m_{hh}$  as electron and hole masses, we obtain a value of 7 meV for the exciton binding energy, which is much too large. The optical effective masses define a convenient set of units which are as follows: (i) momentum unit  $k_F = (3\pi^2 n)^{1/3}$ , where  $n$  is the number of electrons per unit volume; (ii) mass  $\mu$ , the reduced optical mass; (iii) energy  $E_{Ge}^x = \mu e^4 / 2\kappa^2 = 2.65$  (GeV); (iv) density;  $r_s$ , the interparticle

TABLE II. List of band parameters used in calculation.

	$m_l$	$m_t$	$m_{oe}$	$m_{de}$	$A$	$B$	$C$	$m_{lh}$	$m_{hh}$	$\kappa$	$E^x$ (MeV)
Ge	1.58	0.082	0.12	0.22	13.38	8.48	13.15	0.042	0.347	15.36	2.65
Si	0.9163	0.1905	0.26	0.32	4.28	0.75	4.85	0.154	0.523	11.4	12.8
GaAs	0.067	0.067	0.067	0.067	7.65	4.82	7.71	0.074	0.62	12.9	3.62

spacing, is given by  $n^{-1} = \frac{4}{3} \pi r_s^3 a_x^3$ , where  $a_x = \kappa/\mu e^2$ . In these units the kinetic energy per electron in the metallic state is

$$E_k = \frac{3}{5} (E_F^e + E_F^h) \\ = \frac{2.21}{r_s^2} \left[ \frac{\mu}{4^{2/3} m_{de}} + \frac{\mu}{m_{lh}} \left( \frac{1}{1 + (m_{lh}/m_{hh})^{3/2}} \right)^{2/3} \right] \quad (3.9)$$

$$= 0.468/r_s^2. \quad (3.10)$$

The evaluation of the exchange energy is more complicated. First the distribution of the electrons among four ellipsoids leads to a lowering of the exchange energy since only electrons in the same ellipsoid will contribute to the exchange energy. Since the exchange contribution is proportional to the Fermi wave vector there will be a reduction of  $4^{1/3}$  from this effect. Secondly, although the exchange energy does not depend directly on a mass it is weakly dependent on the shape of Fermi surface. Combescot and Nozières have given an elegant analytic derivation of the exchange energy in an ellipsoidal band. Using their result we may write

$$E_{ex}^e = \frac{-3e^2}{4\pi\kappa} k_e \phi(\rho_e) = \frac{-0.916}{r_s} \frac{\phi(\rho_e)}{4^{1/3}}, \quad (3.11)$$

where  $\rho_e = m_t/m_l$  and  $k_e = k_F/4^{1/3}$  in Ge and

$$\phi(\rho) = \rho^{1/6} \frac{\sin^{-1}(1-\rho)^{1/2}}{(1-\rho)^{1/2}} \quad \text{for } \rho < 1. \quad (3.12)$$

In Ge  $\rho_e = 0.0525$  and the correction factor  $\phi = 0.84$ , thus, the anisotropy and degeneracy reduce the exchange energy but by a much smaller amount than in the kinetic energy.

The calculation of the exchange energy for the holes is considerably more complicated. There are matrix elements of the Coulomb interaction between the heavy and light hole bands. The calculation of the exchange energy can be reduced to a four-dimensional integration which has been calculated numerically. The details of the calculation are given in Appendix C and using the result (C3) we have

$$E_{ex}^h = \frac{-0.916}{r_s} \left( \frac{m}{m_v^d} \right)^2 \beta, \quad (3.13)$$

where  $(m_v^d)^{3/2} = m_{lh}^{3/2} + m_{hh}^{3/2}$  and the evaluation of the coefficient  $\beta$  is described in Appendix C. Substituting the values for germanium and combining with the result (3.11) for the electrons, we find the following result for the total exchange energy:

$$E_{ex} = E_{ex}^e + E_{ex}^h = \frac{-0.486}{r_s} - \frac{0.650}{r_s} = -\frac{1.136}{r_s}. \quad (3.14)$$

In the calculation of the correlation energy there will be effects from both the anisotropies and degeneracies in the band structure of Ge. It is

straightforward to incorporate the latter with the modified RPA but not the former. In particular, the complex structure of the hole bands poses a formidable obstacle to a direct evaluation of the RPA. We chose instead to ignore the effects of the anisotropy in the correlation energy and to approximate the band structure by four isotropic electron bands and two isotropic hole bands. As the characteristic mass we chose the optical mass since this mass characterizes the plasma frequency and behavior of  $\epsilon(q, \omega)$  for  $\omega \gg v_F q$  (where  $v_F$  is the Fermi velocity). This is clearly a fairly crude approximation, given the highly anisotropic nature of the bands in Ge, and it will tend to underestimate the correlation energy. CN have chosen to approach the problem in a different way. They have used the Nozières-Pines (NP) approximation to the correlation energy. This is very similar in spirit to Hubbard's modification of the RPA. In the NP approximation the integrand in the final integral over  $k$  in Eq. (2.8) is expanded around the small- and large- $k$  limits. At small  $k$  the RPA result is expanded in powers of  $k$  while for large  $k$  all the second-order diagrams are included. In between a simple interpolation is used. Using this scheme, CN have found it possible to include the effects of the anisotropy. They find that the effect of the anisotropy is to increase the magnitude of the correlation energy by 20% over the isotropic approximation employed here. A detailed discussion of the effects of the anisotropy on the plasmon energy, etc., can be found in their paper.<sup>15</sup>

The calculation of the correlation energy proceeds as outlined in Sec. II with the substitution in Eq. (2.8) of

$$\pi = 4\pi^e + 2\pi^h, \quad A/A' = \Sigma/\Sigma', \\ \Sigma' = 4[1 - k^2/12(k^2 + k_e^2)]\Sigma^e \\ + 2[1 - k^2/12(k^2 + k_F^2/2^{2/3})]\Sigma^h, \quad (3.15)$$

Note that the correction factor for the exchange diagrams is now of only marginal importance and represents only a 3% change in the correlation energy. The angular integrations over  $\vec{k}$  are trivial and one is left with a double integral that can be evaluated numerically. In Table I we quote the results obtained in this way for the correlation energy. Comparing to the values obtained by CN we see that the effect of incorporating the anisotropy is to enhance the correlation by some 20% in the case of Ge. In Fig. 1(b) we plot the total ground-state energy of the electron-hole liquid vs  $r_s$ . The shape of the curve has changed considerably from the isotropic model discussed in Sec. II. There is now a deep minimum at  $r_s = 0.63$  at a value of  $E_G^0 = -2.0$  leading to a binding energy of 1.7 meV relative to the experimental

value of the free-exciton binding energy. In Table III, we list the values obtained by us for the binding energy and equilibrium density and also the values of CN and the experimental values. The latter were determined (a) from the phase diagram studies of Pokrovsky and Svistunova<sup>5</sup> and (b) from the recombination radiation studies of Benoît à la Guillaume, Voos, and Salvan.<sup>35</sup> Since at equilibrium the sum of the chemical potentials

$$\mu_e + \mu_h = \frac{\partial[NE_G(\gamma_s)]}{\partial N} = E_G^0(\gamma_s),$$

the binding energy is given by the difference in energy of the *upper* edge of the shifted recombination and the lower edge of the free-exciton line. The equilibrium density has been determined in a number of ways, as discussed in Ref. 35. Comparing theory and experiment we think that the agreement in regard to the equilibrium density is very good. Our value of the binding energy is smaller than experiment and the incorporation of anisotropy of the band structure in the correlation energy by CN leads to a theoretical value in excellent agreement with experiment.

Finally we wish to remark that at the equilibrium density of  $2 \times 10^{17} \text{ cm}^{-3}$ , the electron density at a hole is already larger, even excluding enhancement factors, than the value in the free exciton of  $1.1 \times 10^{17} - 1.5 \times 10^{17} \text{ cm}^{-3}$ . We estimate the latter from the theoretical calculations of McLean and Loudon.<sup>34</sup>

#### B. Silicon

The band structure of Si is very similar to that of Ge. The main differences are that the bands are much less anisotropic and that there are six electron ellipsoids centered at the set of points obtained from  $(0, 0.85, 0, 0)2\pi/a$ . The calculation of the ground-state energy proceeds in an identical manner. The values of the band-structure parameters used are given in Table II.<sup>31,36</sup> The kinetic energy per electron is given by

$$E_k = \frac{2.21}{\gamma_s^2} \left[ \frac{\mu}{6^{2/3} m_{de}} + \frac{\mu}{m_{hh}} \left( \frac{1}{1 + (m_{lh}/m_{hh})^{3/2}} \right)^{2/3} \right] \quad (3.16)$$

$$= 0.727/\gamma_s^2. \quad (3.17)$$

Using  $k_e = k_F/6^{1/3}$  in Eq. (3.11) and the results of Appendix C, we obtain the exchange energy:

$$E_{ex} = -1.157/\gamma_s. \quad (3.18)$$

In the calculation of the correlation energy the correction of the exchange diagrams now cancels only  $\frac{1}{18}$  of the RPA contribution at short wavelength. The results of the calculation are shown in Fig. 5. The ground-state energy has a minimum at  $\gamma_s = 0.84$  with a value of  $E_G^0 = -1.59$ . This compares with the value of  $-1.60$  for  $E_G^0$  at  $\gamma_s = 0.95$  found by Combescot and Nozières. The agreement between the two methods is much better than in germanium, which is not surprising since the bands in Si are much less anisotropic. This is also the reason why the metallic state is considerably less bound than in Ge. Using the experimental value of  $14.7 \text{ meV}$  for the binding energy of the free exciton found by Shaklee and Nahory,<sup>37</sup> we find a binding energy of  $5.7 \text{ meV}$  for the metallic state. Although Si has not been as extensively studied as Ge, from the optical-luminescence studies of Pokrovsky *et al.*<sup>8</sup> we obtain an experimental value of  $6.8 \text{ meV}$ . The equilibrium density we find is  $3.4 \times 10^{18}$ , in excellent agreement with the value of  $3.7 \times 10^{18}$  estimated in Ref. 8. Overall, as in Ge, the agreement between theory and experiment is strikingly good.

#### C. Ge under a [111] Strain

The application of a uniaxial stress lifts the degeneracies in the band structure.<sup>38</sup> In particular, the application of a stress along a [111] direction raises the energy of the ellipsoids at the other [111] points relative to the ellipsoid at the zone boundary in the direction of the applied stress. In addition, the application of stress lifts the de-

TABLE III. Theoretical and experimental values of the binding energy and equilibrium density.

Binding energy	Ge	Si
This work	1.7 meV	5.7 meV
Combescot and Nozières (Ref. 15)	2.5 meV	6.3 meV
Expt: Pokrovsky and Svistunova (Ref. 5)	2.7 meV	6.8 meV (Ref. 8)
Benoît à la Guillaume <i>et al.</i> (Ref. 35)	2.4 meV	...
Equilibrium density		
This work	$1.8 \times 10^{17} \text{ cm}^{-3}$	$3.4 \times 10^{18} \text{ cm}^{-3}$
Combescot and Nozières (Ref. 15)	$2.0 \times 10^{17} \text{ cm}^{-3}$	$3.1 \times 10^{18} \text{ cm}^{-3}$
Expt: Benoît à la Guillaume <i>et al.</i> (Ref. 35)	$1.95 (\pm 0.65) \times 10^{17} \text{ cm}^{-3}$	...
Pokrovsky <i>et al.</i> (Ref. 8)	$2.6 \times 10^{17} \text{ cm}^{-3}$	$3.7 \times 10^{18} \text{ cm}^{-3}$



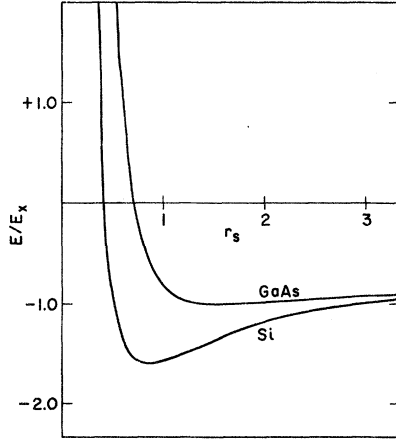


FIG. 5. Ground state of the metallic electron-hole gas in Si and GaAs. The parameters used in the calculation are listed in Table II.

generacy between the valence bands at  $\Gamma$ . In the presence of a fairly large, but readily attainable, value of the stress, the degeneracies are split by a sufficiently large amount that only one band need be considered for the electrons and for the holes. The value of applied stress necessary to reach this limit is estimated at the end of this section. While it is clear that the state with all of the electrons in the ellipsoid with the lowest energy is clearly the ground state of the electron-hole liquid, it is not *a priori* obvious that such a state can be realized experimentally. Since in the excitation processes the electrons will be in  $k$  states near the center of the zone, their decay via optical phonons will distribute them equally between the four ellipsoids. If the intervalley scattering time  $\tau_{1v}$  is sufficiently short  $\tau_{1v} \ll \tau_0$ , where  $\tau_0$  is the decay time of metallic phase then one can assume all of the electrons are in the lowest ellipsoid. At low temperatures, intervalley scattering via zone-boundary phonons will be very unlikely and the dominant contribution to  $\tau_{1v}$  must come from electron-electron scattering. In Appendix D a crude estimate is obtained for  $\tau_{1v}$  and, using the experimental value of  $10^{-5}$  sec for  $\tau_0$ , we find  $\tau_{1v}/\tau_0 \sim 10^{-3}$  sec. Thus we shall make the assumption that all the electrons are in a single ellipsoid.

In the case of hole bands in the presence of a large [111] strain, the upper valence band is ellipsoidal in shape with mass values of  $m/m_1 = A + \frac{1}{3}N$  and  $m/m_t = A - \frac{1}{6}N$  where  $N^2 = 3C^2 + 9B^2$ , leading to values of  $m_1 = 0.04m$  and  $m_t = 0.13m$ . The evaluation of the kinetic energy per electron is straightforward and gives

$$E_k = 1.616/r_s^2. \quad (3.19)$$

In the exchange energy the evaluation proceeds

as before. For the holes we may use Eq. (3.11) with the appropriate expression for  $\phi(\rho)$ :

$$\phi(\rho) = \rho^{1/6} \frac{\sinh^{-1}(\rho-1)^{1/2}}{(1-\rho)^{1/2}}, \quad \rho > 1 \quad (3.20)$$

giving

$$E_{ex} = - (0.916/r_s) [\phi(\rho_e) + \phi(\rho_h)] \quad (3.21)$$

$$= -1.66/r_s. \quad (3.22)$$

The great simplifications make it possible to evaluate the correlation energy exactly within the modified RPA. This is possible because of the simple relationship between the polarizability with the RPA of an ellipsoidal band  $\pi_{RPA}^{e11}$  and that of an appropriately chosen isotropic band. Using the expression (2.6) for  $\pi_{RPA}$ , we note that with the substitution  $p_z^1 = \rho^{1/2} p_z$  and  $q_z^1 = \rho^{1/2} q_z$ , with  $z$  parallel to the longitudinal axis, the integral is the same as for the isotropic band and we get at once

$$\pi_{RPA}^{e11}(k, \omega) = \frac{k'^2}{k^2} \rho^{-1/2} \pi_{RPA}(k', \omega),$$

where  $k'^2 = k_x^2 + k_y^2 + \rho k_z^2$ . The evaluation of the correlation energy can be carried out as before and the extra angular integration required offers no essential complication.

In Fig. 1(c) we plot the results for  $E_G$  vs  $r_s$ . We find a minimum at a value of  $r_s = 1.5$  (or a density of  $1.2 \times 10^{17} \text{ cm}^{-3}$ ) with a value  $E_G^0 = -1.07$ . To our knowledge there are no accurate measurements of the binding energy of the free exciton in the presence of the strain. We can estimate it quite accurately using the theoretical results of Kohn and Luttinger<sup>39</sup> and we find  $E_x = 1.002$ . Within our approximations the metal is bound by a small amount. CN have a value for the ground-state energy slightly smaller than ours and do not find binding. In view of the over-all uncertainties inherent in the RPA no definite theoretical conclusion can be reached.

There are no experimental measurements of the binding energy under strain. Benoit à la Guillaume *et al.*<sup>35</sup> have reported an equilibrium density of  $1.8 \times 10^{17} \text{ cm}^{-3}$  in the presence of a large [111] strain and the persistence of the metallic recombination luminescence. It is possible that the transition to the metallic state occurs under pressure in this case, in analogy with the proposed metallic phase of hydrogen. Clearly, a more detailed experimental investigation of the effect of strain would be of considerable theoretical interest.

#### D. GaAs

We should like to point out that even though the situation is far less clearcut because of fast recombination times, highly excited direct-gap materials will also have their gap renormalized be-

cause of the interaction between the electrons and holes. This point has been emphasized recently by Johnston.<sup>40</sup> Experiments on optically pumped GaAs have exhibited recombination radiation that is shifted toward lower energies in a fashion consistent with the present theory.<sup>17</sup> If one uses the band-structure parameters for GaAs listed in Table II,<sup>41</sup> the same calculations as were discussed for Ge and Si can be performed for this material. Again we assume thermal equilibrium is attained. The results are shown in Fig. 5. The minimum energy is quite close to the exciton binding energy and the density at the minimum corresponds to  $2 \times 10^{16} \text{ cm}^{-3}$ . At the minimum energy, the ground-state energy and the chemical potential are equal so that for this state the recombination radiation should all appear below the exciton line. If one can pump to densities beyond  $2 \times 10^{16} \text{ cm}^{-3}$ , the spontaneous emission will extend over a larger region both above and below the free-exciton line. It should also be noted that at densities higher than those corresponding to the minimum energy of the curves in Fig. 5, the electron-hole gas is under pressure and will attempt to expand rapidly into the lower density regions of the crystal.

#### IV. LOW-DENSITY REGIME

Thus far we have discussed the metallic state and how its energy varies with density, i. e.,  $r_s$ . We now turn to the other extreme, that is, we start at low densities and ask what happens to the excitons as the density increases. The discussion is limited to the model used in Sec. II of isotropic single bands for the electrons and the holes. We make extensive use of the analogy between the case of a hydrogen gas and a gas of excitons. These two systems are simply the extreme limits of the phase diagram obtained from studying a system of electrons and holes with variable mass ratio.

First we consider the interaction between two excitons. Just as for hydrogen atoms, two excitons bind to form a molecule. Of the several calculations<sup>18,42,43</sup> of the binding energy of the positronium or excitonic molecule that have been published, the simplest is that of Hylleraas and Ore,<sup>18</sup> who find that the molecule is bound by  $0.017 E_x$ . The average separation between the two excitons in their wave function is  $\sim 4.5 a_x$ .<sup>44</sup> Comparing this separation to that of the two protons in  $\text{H}_2$ , namely,  $1.5 a_B$ , we see that the excitonic molecule can be thought of as two weakly coupled excitons. The electrons and the holes are separately paired into singlets in this state so that the orbital wave function is nodeless. Any other spin configuration does not lead to binding since their orbital functions must have nodes with the consequent cost in kinetic energy. This state-

ment is also true if one attempts to bind three excitons together to make a larger molecule. Therefore, we need to consider the interaction between two molecules.

The interaction between two hydrogen molecules was first considered by de Boer,<sup>45</sup> whose method we shall follow quite closely. He found that the interaction potential is attractive at distances greater than  $r \sim 5 a_B$  and that there is a weak minimum of  $\sim 10^{-4} \text{ Ry}$  between  $r \sim 5.5 a_B$  and  $6 a_B$ . This weak minimum is responsible for the gas-liquid transition at  $22^\circ \text{K}$  in  $\text{H}_2$ .<sup>46</sup> For two excitonic molecules the situation differs in two ways: (i) Because the separation of the excitons in the molecules is considerably larger, the forces are much more extended and the net attractive force is weaker; (ii) because of the light total masses of the molecules, the weak attractive forces are not sufficient to cause a gas-liquid transition. To verify the first statement we note that the van der Waals forces between two excitons have the same relative magnitude in this problem as in  $\text{H}_2$ , that is, if energies are measured in terms of exciton rydbergs and lengths in exciton radii, then the van der Waals interaction is<sup>47</sup>

$$V_v(r)/E_x = -13 (a_x/r)^6 \quad (4.1)$$

and the factor of 13 is the same as for two hydrogen atoms. The repulsive part of the interaction between two excitons also scales in this fashion, but as discussed later, is slightly larger because of the possibility of exchanging both electrons and holes. Since the molecule is made up of well-separated excitons, the effective interaction between two molecules can be written as the sum of the interactions between the excitons averaged over the positions of the excitons. Because the excitons are much more loosely bound than two hydrogen atoms, this final average spreads out the repulsive region considerably, decreasing the density at which the attractive forces can be effective.

These facts regarding the form of the potential, along with the light mass of the molecules, make it unlikely that a gas-liquid transition will occur for the molecules. This can be seen by considering the theory of quantum effects on gas-liquid transitions by de Boer.<sup>46</sup> He writes the effective 6-12 potential describing the interaction between two molecules in the form

$$V(r) = 4\epsilon \left[ \left( \frac{\sigma}{r} \right)^{12} - \left( \frac{\sigma}{r} \right)^6 \right] \quad (4.2)$$

and then introduces a quantum parameter  $\Lambda \equiv \hbar/\sigma(m\epsilon)^{1/2}$ . By plotting the experimental values of the critical temperature against  $\Lambda$  he found that the critical point for the gas-liquid transition appears to go to zero at  $\Lambda \sim 3.5$ . If we assume

that the interaction between two excitonic molecules is the same as that for  $H_2$  molecules, the quantum parameter  $\Lambda \approx 76$ . That the range of the interaction is actually considerably larger for excitonic molecules is not likely to reduce this number below 3.5. In any case, the attractive forces are only important at very low densities so that we will ignore them entirely and ask at what point the repulsive forces are sufficiently strong to break up the molecular gas.

Presumably, this breakup will occur when the product of the scattering length  $a_s^3$  and the density  $n$  is approximately unity. In order to calculate the scattering length, we must determine the form for the repulsive potential. To do this, we follow the derivation due to de Boer<sup>45</sup> for calculating the repulsive potential between two  $H_2$  molecules. The wave function of the molecule is taken to be of the approximate form

$$\psi_{ab}(1, 2) = f(r_{ab}) (e^{-r_{1a}} e^{-r_{2b}} + e^{-r_{1b}} e^{-r_{2a}}) / 2\pi, \quad (4.3)$$

where the unit of length is again taken to be the exciton radius,  $a$  and  $b$  index the holes, and 1 and 2 index the electrons. Following de Boer we assume that this function is an eigenfunction of the Hamiltonian for the molecule. The total wave function for the two molecules is written as the antisymmetrized product of the above wave function for each molecule. The same approximations made by de Boer of keeping only terms that are lowest order in the overlap integrals is also made here. Let  $H'$  be the sum of the Coulomb interactions between particle ( $a, b, 1, 2$ ) and particles ( $c, d, 3, 4$ ). Then there are three types of terms: (i) the direct Coulomb interaction

$$H'_c = \int \psi_{ab}(12) \psi_{cd}(34) H' \psi_{ab}(12) \psi_{cd}(34) d\tau; \quad (4.4)$$

(ii) the interaction due to the exchange of two electrons

$$H'_{ex} = \int \psi_{ab}(1, 3) \psi_{cd}(2, 4) H' \psi_{ab}(1, 2) \psi_{cd}(3, 4) d\tau; \quad (4.5)$$

(iii) the interaction due to the exchange of two holes

$$H'_{ex}^h = \int \psi_{ac}(1, 2) \psi_{bd}(3, 4) H' \psi_{ab}(1, 2) \psi_{cd}(3, 4) d\tau. \quad (4.6)$$

The first two of these terms reduce to exactly the same expression as obtained by de Boer, only they are averaged over the wave function  $f(r_{ab})$ . If  $C(r)$  and  $J(r)$  are defined as

$$C(r_{ab}) = \frac{1}{\pi^2} \int e^{-2(r_{a1} + r_{b2})} \left( \frac{2}{r_{ab}} - \frac{2}{r_{a2}} - \frac{2}{r_{b1}} + \frac{2}{r_{12}} \right) d^3r_1 d^3r_2 \quad (4.7)$$

and

$$J(r_{ab}) = \frac{1}{\pi^2} \int e^{-2(r_{a1} + r_{a2} + r_{b1} + r_{b2})} \left( \frac{2}{r_{ab}} - \frac{2}{r_{a2}} - \frac{2}{r_{b1}} \right)$$

$$+ \frac{2}{r_{12}} \int d^3r_1 d^3r_2, \quad (4.8)$$

the total contribution from the first two types of terms is

$$H'_c + H'_{ex} = 4 \int d^3R_{ab} d^3R_{cd} f^2(R_{ab}) f^2(R_{cd}) [C(R_{ac}) - \frac{1}{2} J(R_{ac})]. \quad (4.9)$$

In a similar fashion the expression for the exchange of two holes can be reduced to

$$H'_{ex}^h = -2 \int \int d^3R_{ab} d^3R_{cd} f(R_{ab}) f(R_{cb}) \times f(R_{ad}) f(R_{cd}) J(R_{ac}). \quad (4.10)$$

This is similar to the conventional form for the nonlocal exchange interaction with an effective potential  $\frac{1}{2} J(r)$ . Finally we must establish a form for  $f(r)$ . Since we are only interested in the long-range behavior and the best estimate of the molecular binding energy is  $\sim 0.02 E_{xx}$ , the  $f(r)$  is taken to be  $(\pi/\beta^3)^{1/2} e^{-\beta r}$ , where  $\beta = (0.02)^{1/2}$ . In order to carry out the integrals in a relatively simple fashion and obtain a value of the scattering length, we note that  $C(r)$  and  $J(r)$  both drop off as  $e^{-2r}$  at large distances so that the interaction is relatively short ranged on the scale of the function  $f(r)$ . Therefore we replaced both  $C(r)$  and  $J(r)$  by  $\delta$  functions whose weight is determined by their average values. Then carrying out the above integrals for a given value of  $\bar{R} = \frac{1}{2} [\bar{R}_a + \bar{R}_b - \bar{R}_c - \bar{R}_d]$ , we obtain for the total repulsive interaction

$$V(R) = H'_c + H'_{ex} + H'_{ex}^h = \frac{104}{3} \beta^3 e^{-4\beta R} [1 + 4\beta R + \frac{1}{3} (4\beta R)^2]. \quad (4.11)$$

The scattering amplitude  $a_s$  can be obtained approximately from the variational procedure given by Messiah.<sup>46</sup> The result is

$$a_s = 6.9 a_x. \quad (4.12)$$

The description of the molecular state in terms of a weakly interacting gas of molecules breaks down at  $r_s \approx a_s$ . This presumably means that the energy gained by the formation of molecules is overcome by the repulsive interactions around  $r_s = 7$  and the ground-state energy begins to increase. If this increase is rapid enough then one can satisfy the conditions for obtaining a first-order transition to the metallic state as illustrated in Fig. 6. This transition would be similar to the proposed metal-insulator transition in  $H_2$  but with a larger volume change. It is, of course, possible that before one changes to the metallic state the molecular state is destroyed and some form of excitonic state is formed.<sup>21</sup> This point is discussed further in Sec. V.

In conclusion we should like to comment on how the considerations of this section can be extended

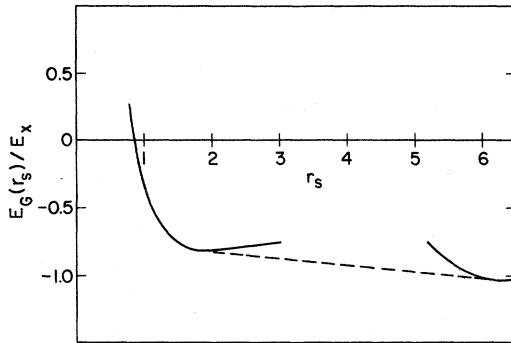


FIG. 6. Possible phase diagram for the isotropic band model. The solid curve on the left is the ground-state energy vs  $r_s$  of the metallic state, while the right-hand curve is a suggested curve based on the low-density considerations in Sec. IV. The dashed line thus represents a first-order change between the low- and high-density states.

to more complicated band structures. It is not expected that anisotropy of the bands alone can change the sign of the scattering length and modify our conclusions. For degenerate bands it may be possible to bind larger complexes since the exclusion principle does not enter until one has complexes with more than two particles per subband. Whether infinitely large complexes can be formed in such a way that the repulsive interactions due to the exclusion principle are overcome by a suitable choice of geometry is not clear.

#### V. RELATION TO THE THEORY OF METAL-INSULATOR TRANSITIONS

In recent years there has been considerable theoretical interest in the transition at low temperatures between metallic and semiconducting phases. It was suggested by Mott<sup>49</sup> that such a transition must be intrinsically first order at zero temperature because of the long-range Coulomb forces between electrons and holes in semiconductors. Subsequently the problem (reviewed in Refs. 20 and 21) of an uncrossing of overlapping bands was examined in detail by a number of investigators using a Hartree-Fock approximation. They found that near zero-energy gap a sequence of excitonic phases characterized by spin or charge density waves could be stable. These phases were bounded on the semiconducting side by the condition that the binding energy of a single exciton is greater than the (indirect) energy gap. The excitonic phase relieves the instability towards the creation of a large number of excitons by introducing a pairing in the ground state between electrons and holes.<sup>20,21</sup> Within the Hartree-Fock approximation the interaction between excitons is repulsive and hence the excitonic state

is stable. However, as already mentioned, two excitons are known to bind so that Hartree-Fock theory cannot be correct.<sup>50</sup>

It was pointed out by Halperin and Rice,<sup>21</sup> that the study of the excitonic instability reduces to the study of an electron-hole gas at a constant chemical potential. That is, instead of studying a system of electrons and holes at a constant density, as we have been doing in this paper, one considers a variable number of electrons and holes but adds a term  $H' = (E_G/2)(N_e + N_h)$  to the Hamiltonian in Eq. (2.1) to represent the gap. This term acts like a negative chemical potential. The proposition that excitonic phases occur near zero gap is equivalent to the proposition that in the electron-hole gas a Bose condensed phase of excitons is the stable phase at some value of the chemical potential. We have seen in this paper that in semiconductors such as Ge and Si where there is considerable anisotropy and degeneracy in the band structure that the state with minimum energy at zero temperature is the metallic liquid. Therefore, for such semiconductors if one reduces the indirect energy gap continuously, a first-order transition occurs directly to the metallic phase, bypassing all excitonic phases. The transition occurs when the energy gap is equal to the ground-state energy per particle of the metallic phase. In such a case we would expect a phase diagram of the form shown in Fig. 7, where the critical temperature  $T_c$  is that for the liquid-gas transition in the electron-hole system.

If the energy bands are only slightly anisotropic and are not degenerate, our calculations indicate the metallic state is not the state of minimum chemical potential but rather, as discussed in Sec. IV, the molecular state. Under such circumstances the theory discussed in Refs. 20 and 21 may be applicable. The excitonic or Bose condensed phase may be stable as the chemical potential increases and the molecular correlations between excitons become unimportant. The ex-

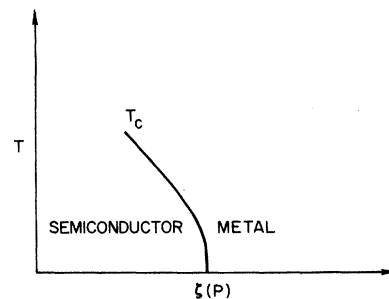


FIG. 7. Expected phase diagram for the metal insulator transition. The transition is first order with the order parameter the density of electrons in the conduction bands.

citon-exciton interactions are then effectively repulsive. However, the final transition to the metallic state is likely to be first order since the band structure in the intermediate excitonic phase may be expected to have multiple extrema and to be anisotropic. Thus it would seem unlikely that a series of excitonic phase changes will occur. In conclusion it should be remarked that the experiments in Ge are relevant to the considerations of metal-insulator transitions in that they confirm experimentally for the first time the idea that the density of electrons *in a given band* can be used as a bonafide order parameter to describe a phase transition. This idea has been the basic assumption in the area of excitonic insulators and much of the work on the Mott transition.

#### ACKNOWLEDGMENTS

The authors would like to acknowledge stimulating and helpful correspondence with P. Nozières and M. Combescot. We would also like to thank P. W. Anderson, J. C. Hensel, and T. G. Phillips for several discussions, and S. T. Chui for doing some preliminary calculations in the early stages of this work.

#### APPENDIX A: $t$ -MATRIX CALCULATION

In order to estimate the importance of the multiple scattering of an electron and a hole we calculate the bound-state energy of an electron and a hole interacting via the screened Coulomb interaction. For isotropic bands this binding energy is nonzero for all values of  $r_s$  and its value was previously discussed in the high-density limit by Kozlov and Maksimov.<sup>28</sup> Let  $\psi(k)$  be the Fourier transform of the electron-hole-pair wave function with binding energy  $\omega$  measured relative to the sum of the Fermi energies of the electrons and holes.  $\psi(k)$  must satisfy the equation<sup>51</sup>

$$\left[ \frac{2}{m} (k^2 - k_F^2) \psi(k) - 4\pi e^2 \int_{k' > k_F} \frac{d^3 k'}{(2\pi)^3} \times \frac{1}{(|\vec{k} - \vec{k}'|^2 + k_{FT}^2)} \psi(k') \right] = \omega \psi(k). \quad (\text{A1})$$

We have tried several types of variational solutions to this equation and have found that there are two regimes depending on whether  $r_s \gtrless 7.5$ . If  $r_s$  is less than 7.5 we find only a Cooper-pair-type solution and we use a trial function

$$\psi_1(k) = A/k(k^2 - \beta^2). \quad (\text{A2})$$

Here the  $k$  in the denominator is introduced instead of a high-energy cutoff and  $\beta$  is to be determined variationally. The only solutions with this trial function are those with  $\beta$  nearly equal to unity and we can expand the energy in powers of

$1 - \beta k_F^{-1} \equiv \delta$ . We find that

$$\bar{\omega} = -4\delta[a \ln^2(\delta) + b \ln \delta], \quad (\text{A3})$$

where

$$\bar{\omega} \equiv \frac{\omega}{k_F^2/2m}, \quad a = \frac{1}{4} \lambda \ln \left( \frac{4 + \nu^2}{\nu^2} \right), \quad (\text{A4})$$

and

$$b = 1 - \frac{1}{2} \lambda \left[ \ln 2 \ln \left( \frac{4 + \nu^2}{\nu^2} \right) + \int_0^1 dx \ln \left( \frac{1-x}{1+x} \right) \frac{d \ln \left( \frac{(1+x)^2 + \nu^2 x^2}{(1-x)^2 + \nu^2 x^2} \right)}{dx} \right]. \quad (\text{A5})$$

Here  $\nu^2 = k_{FT}^2/k_F^2$  and the dimensionless coupling constant  $\lambda = \nu^2/8$ . Minimizing  $\bar{\omega}$  with respect to  $\delta$  we find the energies plotted on the enlarged scale in Fig. 8. We see that the binding energy in this region of  $r_s$  varies from  $2 \times 10^{-4}$  ( $k_F^2/2m$ ) to  $10^{-2}$  ( $k_F^2/2m$ ).

A slightly better trial function for larger  $r_s$  is

$$\psi_2(k) = \frac{A}{k^2(k^2 - \beta^2)}. \quad (\text{A6})$$

This function has essentially the same properties as  $\psi_1$  for small  $r_s$  but develops a second minimum at  $\beta = 0$  at  $r_s \simeq 7.5$ . Above  $r_s = 8.2$  the minimum energy switches over to  $\beta = 0$ . The  $\beta = 0$  values for this function are the dashed line in Fig. 8. Above  $r_s = 7.5$  it is more profitable to use a hydrogenic-type solution of the form

$$\psi_3 = \frac{A_3}{(k^2 + \beta^2)^2}. \quad (\text{A7})$$

The minimum energy for  $\psi_3$  is plotted as the solid line in Fig. 8. We see that the state moves out of the continuum, i. e.,  $\bar{\omega} < -2$  at  $r_s = 10.5$ . This

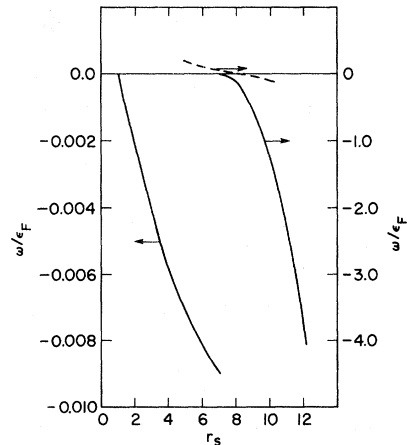


FIG. 8. Calculation of the binding energy of an electron and a hole using various approximate wave functions. The high-density curve was obtained using the wave function (A2), the dashed line (A6), and the low-density curve (A7).

is quite close to the Mott criteria, which does not include the orthogonality to the Fermi sea contained in Eq. (A1).

It should be noted that for  $r_s < 7.5$  the superconducting-type instability contributes a total energy of order  $\omega^2/\epsilon_F$  to the binding energy of the metal since only a fraction  $\omega$  of the electrons and holes are involved in the pairing. Therefore we conclude that the contribution to the ground-state energy due to the formation of electron-hole pairs is quite small in the regime of interest.

#### APPENDIX B: ELECTRON-HOLE CORRELATION FUNCTION IN RPA

In a multicomponent system we can define a function  $g^{\alpha\beta}(r)$  that gives the probability of finding a particle of type  $\alpha$  a distance  $r$  from a particle of type  $\beta$ , in terms of the corresponding correlation function  $S^{\alpha\beta}(q, t)$ <sup>25</sup>

$$g^{\alpha\beta}(\vec{r}) - 1 = \frac{1}{n^\alpha n^\beta} \int \frac{d^3q}{8\pi^3} e^{i\vec{r}\cdot\vec{q}} S^{\alpha\beta}(q, 0), \quad \alpha \neq \beta \quad (\text{B1})$$

where  $n^\alpha$  and  $n^\beta$  denote the densities of particles of type  $\alpha$  and  $\beta$ , respectively. The function  $S^{\alpha\beta}(q, t)$  is defined as

$$S^{\alpha\beta}(\vec{q}, t) = \langle \psi_0 | \rho_{\vec{q}}^\alpha(t) \rho_{-\vec{q}}^\beta(0) | \psi_0 \rangle, \quad (\text{B2})$$

where  $\rho_{\vec{q}}^\alpha(t)$  is the Fourier transform of the density operator in the Heisenberg representation of the particles of type  $\alpha$ . Using the relation between the correlation function and the corresponding dielectric function

$$\zeta_\alpha^{-1} \zeta_\beta^{-1} \text{Im}\epsilon^{-1}(\vec{q}, \omega) = (2\pi e^2/q^2) [S^{\alpha\beta}(q, -\omega) - S^{\alpha\beta}(q, \omega)], \quad (\text{B3})$$

where  $\zeta_\alpha = -1$  if  $\alpha$  is an electron and  $\zeta_\alpha = +1$  if  $\alpha$  is a hole, we obtain the result

$$S^{\alpha\beta}(\vec{q}, 0) = \frac{1}{\zeta_\alpha \zeta_\beta} \frac{q^2}{4\pi^2 e^2} \int_0^\infty d\omega \text{Im} [\epsilon_{\alpha\beta}^{-1}(\vec{q}, \omega)]. \quad (\text{B4})$$

The dielectric function  $\epsilon_{\alpha\beta}$  which relates the induced particle density of type  $\alpha$  to the perturbing potential acting on the particle density of type  $\beta$  is given simply within the RPA, for  $\alpha \neq \beta$ , by

$$\frac{1}{\epsilon_{\alpha\beta}(\vec{q}, \omega)} = \frac{\pi_{\text{RPA}}^\alpha(q, \omega) \pi_{\text{RPA}}^\beta(\vec{q}, \omega)}{1 - [\pi_{\text{RPA}}^\alpha(\vec{q}, \omega) + \pi_{\text{RPA}}^\beta(\vec{q}, \omega)]} \quad (\text{B5})$$

$$= \frac{\pi_{\text{RPA}}^\alpha(q, \omega)}{1 - 2\pi_{\text{RPA}}^\alpha(q, \omega)}, \quad (\text{B6})$$

in the isotropic single-band equal-mass electron-hole liquid. If we express  $\pi_{\text{RPA}}$  in terms of the dimensionless variables  $x = q/k_F$  and  $y = \omega/E_F$ , then we can write

$$\begin{aligned} \pi_{\text{RPA}}(q, \omega) &= (e^2 m/k_F) F(x, y) \\ &= 2\alpha_0 r_s F(x, y), \end{aligned} \quad (\text{B7})$$

where  $\alpha_0 = (4/9\pi)^{1/3}$ .

Substituting in (B1) we obtain the result

$$\begin{aligned} g^{\alpha\beta}(\vec{r}) - 1 &= \frac{k_F^5 E_F}{n^\alpha n^\beta \zeta_\alpha \zeta_\beta 4\pi^2 e^2} \int \frac{d^3\vec{x} x^2 e^{i\vec{x}\cdot\vec{r}k_F}}{8\pi^3} \\ &\quad \times \int_0^\infty dy \frac{4\alpha_0^2 r_s^2 F^2(x, y)}{1 - 4\alpha_0 r_s F(x, y)} \quad (\text{B8}) \\ &= \frac{9\alpha_0 r_s}{32\pi \zeta_\alpha \zeta_\beta} \int d^3x x^2 e^{i(\vec{x}\cdot\vec{r}k_F)} \int_0^\infty dy \frac{F^2(x, y)}{1 - 4\alpha_0 r_s F(x, y)}. \end{aligned} \quad (\text{B9})$$

The expression (B9) is very similar to that used to calculate the correlation function  $g^{hh}(r)$  for electrons of opposite spins in the single-component electron gas. The integrand of Eq. (B9) is the same as in  $g^{hh}(r)$  if we replace the coefficient  $4\alpha_0 r_s$  in the denominator by  $\alpha_0 r_s$ . Thus we can scale the results for the electron gas at a value of  $r_s = 1$  in Bohr radii, to the electron-hole gas at  $r_s = 4$  in exciton units by multiplying the answer by  $\frac{1}{2}$ . Using the results of Lobo *et al.*,<sup>52</sup> who calculated  $g^{hh}(r)$  within the RPA for the electron gas, we obtain the curve for  $g^{\text{eh}}(r)$  at a value of  $r_s = 1$ .

The results in Fig. 4 show an enhancement of approximately a factor of 2 at the origin. If we use the results of Ref. 51 and extrapolate to  $r_s = 2$  we find an enhancement of  $g^{\text{eh}}(r)$  of approximately a factor of 3 at the equilibrium value of  $r_s$ .

#### APPENDIX C: VALENCE-ELECTRON EXCHANGE

In order to calculate the exchange between the valence-band holes we must take into account the detailed nature of the wave functions near the valence-band edge. The exchange energy including the effect of these wave functions can be written as

$$\begin{aligned} E_{\text{ex}} &= \frac{1}{2} \frac{e^2}{\epsilon} \sum_{n, n'}^{\text{occ}} \int_{S_n} \frac{d^3k}{(2\pi)^3} \int_{S_{n'}} \frac{d^3k'}{(2\pi)^3} \frac{4\pi}{|\vec{k} - \vec{k}'|^2} \\ &\quad \times |\langle \phi_{\vec{k}n} | \phi_{\vec{k}'n'} \rangle|^2. \end{aligned} \quad (\text{C1})$$

Here the integrals over  $\vec{k}$  and  $\vec{k}'$  are restricted to the occupied regions of the bands  $n$  and  $n'$ . The  $\phi_{\vec{k}n}$  are the wave functions at  $\vec{k}$  which are written in terms of the wave functions at  $\vec{k}=0$  by the  $\vec{k}\cdot\vec{p}$  method.<sup>53</sup> For Ge there are four bands which are degenerate in pairs, so that the occupied region is determined by two Fermi surfaces. In order to reduce (C1) to a convenient expression for computation, we measure all momenta in units of  $k_F = (2m\epsilon_F/\hbar^2)^{1/2}$ . Then dividing by the density  $n \equiv (m_v^a/m)^{3/2} k_F^3/3\pi^2$  and measuring energies in units of  $E_x$ , we have

$$\begin{aligned} \frac{E_{\text{ex}}^h}{nE_x} &= 3\pi^2 \left(\frac{m}{m_v^a}\right)^{3/2} (k_F a) \left( \sum_{nn'}^{\text{occ}} \int_{S_n} \frac{d^3k}{(2\pi)^3} \int_{S_{n'}} \frac{d^3k'}{(2\pi)^3} \right. \\ &\quad \left. \times \frac{4\pi}{|\vec{k} - \vec{k}'|^2} |\langle \phi_{\vec{k}n} | \phi_{\vec{k}'n'} \rangle|^2 \right), \end{aligned} \quad (\text{C2})$$

where the momentum variables are in units of  $k_F$ . Substituting for  $(k_F a)$  in terms of  $r_s$  gives

$$\frac{E_{ex}^h}{nE_x} = \left[ \frac{3}{2\pi} \left( \frac{9\pi}{4} \right)^{1/3} \frac{1}{r_s} \right] \left( \frac{m}{m_v^a} \right)^2 \beta, \quad (C3)$$

where

$$\beta \equiv 2\pi^3 \sum_{n, n'}^{\text{occ}} \int_{S_n} \frac{d^3 \vec{k}}{(2\pi)^3} \int_{S_{n'}} \frac{d^3 k'}{(2\pi)^3} \frac{4\pi}{|\vec{k} - \vec{k}'|^2} |\langle \phi_{\vec{k}n} | \phi_{\vec{k}'n'} \rangle|^2. \quad (C4)$$

The product  $\beta(m/m_v^a)^2$  represents the correction to the exchange energy from its value for the isotropic single-band model. In calculating (C4) considerable simplification can be obtained by using the fact that

$$\sum_{n'=1}^4 |\langle \phi_{\vec{k}n} | \phi_{\vec{k}'n'} \rangle|^2 = 1. \quad (C5)$$

Use of this fact allows us to distinguish three regions of integration, depending on whether  $\vec{k}$  and  $\vec{k}'$  are inside the smaller of the two Fermi surfaces  $S_1$ . In region I,  $\vec{k}$  and  $\vec{k}'$  are both inside  $S_1$  and the sum over  $n$  and  $n'$  of the matrix element adds up to 4. In region II, either  $\vec{k}$  or  $\vec{k}'$  but not both is inside  $S_1$  and the sum over  $n$  and  $n'$  adds up to 2. In region III neither  $\vec{k}$  nor  $\vec{k}'$  is inside  $S_1$  and the matrix element must be calculated explicitly. We have calculated these matrix elements by calculating the eigenfunctions of the  $4 \times 4$   $\vec{k} \cdot \vec{p}$  matrix given in the review article by Kohn.<sup>53</sup> We need only the eigenfunctions for the heavy-mass band. After considerable algebra we find that

$$\sum_{n, n'=1}^2 |\langle \phi_{\vec{k}n} | \phi_{\vec{k}'n'} \rangle|^2 = 2 \{ 1 + (1/XX') [(\frac{1}{2}P - E)(\frac{1}{2}P' - E') \times (RR'^* + R^*R' + S^*S' + SS'^*) - (\frac{1}{2}P - E)^2 (|R'|^2 + |S'|^2) - (\frac{1}{2}P' - E')^2 (|R|^2 + |S|^2)] \}. \quad (C6)$$

Here  $P, S,$  and  $R$  are the same functions of  $\vec{k}$  defined by Kohn. The primed functions are these same functions with  $\vec{k}'$  replacing  $\vec{k}$ . The variable  $E$  is the energy of the state  $\vec{k}n$  and  $X$  is defined to be

$$X = (\frac{1}{2}P - E)^2 + |R|^2 + |S|^2. \quad (C7)$$

The expression (C6) depends only on the angles  $\vec{k}$  and  $\vec{k}'$  make with respect to the cubic axes. Therefore we can perform the integrations over the magnitude of  $\vec{k}$  and  $\vec{k}'$  in Eq. (C4) for  $\beta$ . If  $k_1(\theta, \phi)$  and  $k_2(\theta, \phi)$  are the magnitudes of the Fermi momenta in the direction  $(\theta, \phi)$  for the smaller and larger Fermi seas, respectively, we can write  $\beta$  as

$$\beta = \frac{1}{8\pi^2} \left( \int d\Omega d\Omega' I(k_1, k_1') |\phi|^2 + 2 \int d\Omega d\Omega' I(k_2, k_1') \times (2 - |\phi|^2) + \int d\Omega d\Omega' I(k_2, k_2') |\phi|^2 \right), \quad (C8)$$

where  $|\phi|^2$  is defined to be the expression (C6) and

$$I(k_i k_j) \equiv \int_0^{k_i} k^2 dk \int_0^{k_j} k'^2 \frac{dk'}{k'^2 + k^2 - 2k'k\mu}, \quad (C9)$$

where  $\mu$  is the angle between  $\vec{k}$  and  $\vec{k}'$ . Performing the above integrals we obtain

$$I(k_i, k_j) = \frac{1}{4} \left\{ (k_i k_j^3 + k_i^3 k_j) + \mu \left[ k_i^4 \ln \left( \frac{k_i^2 + k_j^2 - 2k_i k_j \mu}{k_i^2} \right) + k_j^4 \ln \left( \frac{k_i^2 + k_j^2 - 2k_i k_j \mu}{k_j^2} \right) \right] + \frac{2\mu^2 - 1}{(1 - \mu^2)^{1/2}} \times \left[ k_i^4 \tan^{-1} \left( \frac{k_j(1 - \mu^2)^{1/2}}{k_i - k_j \mu} \right) + k_j^4 \tan^{-1} \left( \frac{k_i(1 - \mu^2)^{1/2}}{k_j - k_i \mu} \right) \right] \right\}.$$

The remaining integrals over the four angular variables in Eq. (C8) have been carried out numerically.

The integrand that is obtained after one of the  $\Omega$  integrals has been performed has been found to be a slowly varying function with respect to the final  $\Omega$  variables. This allows one to use a small number of mesh points in the final integration. The results appear to be accurate to three significant figures. Using the parameters in Table II, we determined  $\beta$  to be 0.0903 for Ge and 0.249 for Si.

#### APPENDIX D: INTERVALLEY SCATTERING TIME

Consider the situation in the presence of the strain field that has split off one ellipsoid by an energy  $\Delta$  relative to the other ellipsoids. Since in the excitation process the electrons are promoted to high-energy states mostly in the center of the zone, it is reasonable to assume that the populations in all the ellipsoids are equal after the initial decay via optical and acoustic phonons. We therefore take as our initial state one in which there are equal numbers of electrons in all four ellipsoids (in the case of Ge). Now we are interested in the situation in moderate strains and densities so that  $\Delta$  and  $E_F^i$  (the initial Fermi energy relative to the bottom of the ellipsoid) are much smaller than the energy of a zone-boundary phonon. Therefore, there can be no transfer of electrons between the ellipsoids by emission of phonons and, since we are at low temperatures, by absorption of phonons either. However, it is possible to relax the distribution by electron-electron scattering and we shall now proceed to calculate this rate.

If we take an applied strain along (111) and consider an electron in the ellipsoid at (11 $\bar{1}$ ), for example, it can scatter with an electron in (111) and transfer to (111) or ( $\bar{1}$ 1 $\bar{1}$ ). The rate can be calculated using Fermi's "golden rule" and for  $\Delta \gg E_F^i$  is given by

$$\frac{\partial n_{11\bar{1}}}{\partial t} = -4\pi n_{11\bar{1}} n_{\bar{1}\bar{1}\bar{1}} N(\Delta) I^2, \quad (D1)$$

where  $n_{\bar{1}\bar{1}\bar{1}}$  is the density of electrons in the  $(\bar{1}\bar{1}\bar{1})$  ellipsoid,  $N(\Delta)$  is the density of states of an electron at energy  $\Delta$  from the bottom of the ellipsoid, and  $I$  is the matrix element for scattering. To estimate  $I$  we use a single symmetrized combination of plane waves of  $L_1$ -type symmetry for the wave function and find

$$I = \frac{12\pi e^2}{90\bar{\kappa}(\pi/a)^2},$$

where  $\bar{\kappa}$  is the average dielectric constant at large

wave vector. Following Penn<sup>54</sup> we take  $\bar{\kappa} \approx 2$ .

Solving Eq. (D1) we find by using  $\bar{1}\bar{1}\bar{1} = 11\bar{1}$  and  $n_{\bar{1}\bar{1}\bar{1}}(t) = n_{11\bar{1}}(t)$  that

$$\frac{\partial n_{11\bar{1}}}{\partial t}(t) = -\frac{n_{11\bar{1}}(t)^2}{\tau n_{11\bar{1}}(t=0)}, \quad (D2)$$

with  $\tau \approx 2.5 \times 10^{-9}$  sec for  $\Delta = 20$  meV. Solving for  $n(t)$  we find

$$n_{11\bar{1}}(t) = n_{11\bar{1}}(t=0)\tau/(t+\tau) \quad (D3)$$

so that after 1  $\mu$ sec,  $n_{11\bar{1}}$  has dropped by a factor of  $\approx 400$  from the starting value of  $5 \times 10^{16}$  cm<sup>-3</sup> and is negligible.

<sup>1</sup>L. V. Keldysh, in *Proceedings of the Ninth International Conference on the Physics of Semiconductors, Moscow, 1968*, edited by S. M. Ryvkin and V. V. Shmashov (Nauka, Leningrad, 1968), p. 1303.

<sup>2</sup>V. M. Asnin and A. A. Rogachev, *Zh. Eksp. Teor. Fiz. Pis'ma Red.* **9**, 415 (1969) [JETP Lett. **9**, 248 (1969)].

<sup>3</sup>Y. E. Pokrovsky and K. I. Svistunova, *Zh. Eksp. Teor. Fiz. Pis'ma Red.* **9**, 453 (1969) [JETP Lett. **9**, 261 (1969)].

<sup>4</sup>The first experimental observation of the shifted radiation in Si was by J. R. Haynes [Phys. Rev. Lett. **17**, 860 (1966)].

<sup>5</sup>Y. E. Pokrovsky and K. I. Svistunova, *Fiz. Tekh. Poluprovodn.* **4**, 491 (1970) [Sov. Phys.-Semicond. **4**, 409 (1970)].

<sup>6</sup>A. S. Kaminsky and Y. E. Pokrovsky, *Zh. Eksp. Teor. Fiz. Pis'ma Red.* **11**, 381 (1970) [JETP Lett. **11**, 255 (1970)].

<sup>7</sup>C. Benoît à la Guillaume, F. Salvan, and M. Voos, *J. Lumin.* **1**, 315 (1970).

<sup>8</sup>Y. E. Pokrovsky, A. Kaminsky, and K. Svistunova, in *Proceedings of the Tenth International Conference on the Physics of Semiconductors, Cambridge, Mass., 1970*, edited by S. P. Keller, J. C. Hensel, and F. Stern, CONF-700501 (U. S. AEC Division of Tech. Information, Springfield, Va., 1970), p. 504.

<sup>9</sup>V. M. Asnin, A. A. Rogachev, and N. I. Sablina, *Zh. Eksp. Teor. Fiz. Pis'ma Red.* **11**, 162 (1970) [JETP Lett. **11**, 99 (1970)].

<sup>10</sup>C. Benoît à la Guillaume, M. Voos, F. Salvan, J. M. Laurant, and A. Bonnot, *C.R. Acad. Sci. B* **272**, 236 (1971).

<sup>11</sup>Y. E. Pokrovsky and K. I. Svistunova, *Zh. Eksp. Teor. Fiz. Pis'ma Red.* **13**, 297 (1971) [JETP Lett. **13**, 212 (1971)].

<sup>12</sup>A brief account of this work was given in W. F. Brinkman, T. M. Rice, P. W. Anderson, and S. T. Chui, *Phys. Rev. Lett.* **28**, 961 (1972).

<sup>13</sup>L. J. Sham and T. M. Rice, *Phys. Rev.* **144**, 708 (1966).

<sup>14</sup>J. Hubbard, *Proc. R. Soc. Lond. A* **243**, 336 (1957).

<sup>15</sup>M. Combescot and P. Nozières, *J. Phys. C* **5**, 2369 (1972).

<sup>16</sup>P. Nozières and D. Pines, *Phys. Rev.* **111**, 442 (1958).

<sup>17</sup>K. L. Shaklee (private communication).

<sup>18</sup>E. A. Hylleraas and A. Ore, *Phys. Rev.* **71**, 493 (1947).

<sup>19</sup>N. F. Mott, *Rev. Mod. Phys.* **40**, 677 (1968).

<sup>20</sup>W. Kohn, in *Many-Body Physics*, edited by C. deWitt and R. Balian (Gordon and Breach, New York, 1968), p. 351.

<sup>21</sup>B. I. Halpern and T. M. Rice, *Solid State Phys.* **21**, 115 (1968).

<sup>22</sup>E. Wigner and H. B. Huntington, *J. Chem. Phys.* **3**, 764 (1935).

<sup>23</sup>E. G. Brovman, Y. Kagan, and A. Holas, *Zh. Eksp. Teor. Fiz.* **61**, 2492 (1971) [Sov. Phys.-JETP **34**, 1300 (1972)].

<sup>24</sup>E. Hanamura, in Ref. 8, p. 487.

<sup>25</sup>D. Pines and P. Nozières, *The Theory of Quantum Liquids I* (Benjamin, New York, 1966), p. 335.

<sup>26</sup>R. Kronig, J. de Boer, and J. Koringa, *Physica (The Hague)* **12**, 245 (1946).

<sup>27</sup>N. F. Mott, *Philos. Mag.* **6**, 287 (1961).

<sup>28</sup>A. N. Kozlov and L. A. Maksimov, *Zh. Eksp. Teor. Fiz.*

**48**, 1184 (1965) [Sov. Phys.-JETP **21**, 790 (1965)].

<sup>29</sup>A. Sjolander and M. J. Stott, *Phys. Rev. B* **5**, 2109 (1972).

<sup>30</sup>H. L. Weisberg and S. Berko, *Phys. Rev.* **154**, 249 (1968).

<sup>31</sup>G. Dresselhaus, A. F. Kip, and C. Kittel, *Phys. Rev.* **98**, 368 (1955).

<sup>32</sup>J. C. Hensel and K. Suzuki, in Ref. 8, p. 541.

<sup>33</sup>E. F. Gross, V. I. Safarov, A. N. Titkov, and I. S. Shlimak, *Zh. Eksp. Teor. Fiz. Pis'ma Red.* **13**, 332 (1971) [JETP Lett. **13**, 235 (1971)].

<sup>34</sup>T. P. McLean and R. Loudon, *J. Phys. Chem. Solids* **13**, 1 (1960).

<sup>35</sup>C. Benoît à la Guillaume, M. Voos, and F. Salvan, *Phys. Rev. B* **5**, 3079 (1972); C. Benoît à la Guillaume and M. Voos (unpublished).

<sup>36</sup>J. C. Hensel and G. Feher, *Phys. Rev.* **129**, 1041 (1963).

<sup>37</sup>K. L. Shaklee and R. E. Nahory, *Phys. Rev. Lett.* **24**, 942 (1970).

<sup>38</sup>V. S. Bagaev, T. I. Galkina, and O. V. Gogolin, in Ref. 8, p. 500.

<sup>39</sup>W. Kohn and J. M. Luttinger, *Phys. Rev.* **97**, 1721 (1955); *Phys. Rev.* **98**, 915 (1955).

<sup>40</sup>W. D. Johnston, in *Seventh International Quantum Electronics Conference, Digest of Tech. Papers* (IEEE, London, 1972), p. 14.

<sup>41</sup>In these calculations we use the values deduced by P. Lawaetz [Phys. Rev. B **4**, 3460 (1971)].

<sup>42</sup>R. R. Sharma, *Phys. Rev.* **170**, 770 (1968); *Phys. Rev.* **171**, 36 (1968).

<sup>43</sup>O. Akimoto and E. Hanamura, *Solid State Commun.* **10**, 253 (1972).

<sup>44</sup>A. Ore, *Phys. Rev.* **71**, 913 (1947).

<sup>45</sup>J. de Boer, *Physica (Utr.)* **9**, 363 (1942).

<sup>46</sup>J. de Boer, in *Progress in Low Temperature Physics*, edited by C. J. Gorter (North-Holland, Amsterdam, 1957), Vol. II, p. 1.

<sup>47</sup>G. Herzberg, *Molecular Spectra and Molecular Structure*, 2nd ed. (Van Nostrand, New York, 1950), p. 378.

<sup>48</sup>A. Messiah, *Quantum Mechanics* (North-Holland, Amsterdam, 1966), p. 856.

<sup>49</sup>N. F. Mott, *Proc. Phys. Soc. Lond.* **62**, 416 (1947).

<sup>50</sup>Recently, P. W. Anderson, S. T. Chui, and W. F. Brinkman [J. Phys. C **5**, L119 (1972)] argued that the inclusion of certain polarizability terms outside of Hartree-Fock theory changes the average interaction from repulsive to attractive. As can be seen from the calculations in Sec. III, such considerations are incomplete.

<sup>51</sup>A. K. Rajagopal and C. K. Majumdar, *J. Math. Phys. Sci.* **4**, 109 (1970)

<sup>52</sup>R. Lobo, K. S. Singwi, and M. P. Tosi *Phys. Rev.* **186**, 470 (1969).

<sup>53</sup>W. Kohn, in *Solid State Physics*, edited by F. Seitz and D. Turnbull (Academic, New York, 1957), Vol. 5, p. 257.

<sup>54</sup>D. R. Penn, *Phys. Rev.* **128**, 2093 (1962).